

Competition between loss channels in quantum-dot cavity systems: unconventional consequences

A. Vagov^{1,*}, M. Glässl¹, M. D. Croitoru^{1,2}, V. M. Axt¹, and T. Kuhn³

¹*Institut für Theoretische Physik III, Universität Bayreuth, 95440 Bayreuth, Germany*

²*Departement Fysica, Universiteit Antwerpen, Groenenborgerlaan 171, B-2020 Antwerpen, Belgium and*

³*Institut für Festkörpertheorie, Westfälische Wilhelms-Universität Münster, Germany*

(Dated: August 21, 2018)

We demonstrate that in quantum-dot cavity systems, the interplay between acoustic phonons and photon losses introduces novel features and characteristic dependencies in the system dynamics. In particular, the combined action of both loss mechanisms strongly affects the transition from the weak to the strong coupling regime as well as the shape of Mollow-type spectra in untypical ways. For weak coupling, where the spectra degenerate to a single line, we predict that their widths decrease with rising temperature.

High quality quantum dot (QD) cavity systems allow the realization of various technologically important devices such as sources for single [1] or entangled photons [2], that are relevant for applications in quantum information processing [3] as well as for tests of fundamental aspects of quantum mechanics [4]. As state-of-the-art cavities [5] have now reached a quality, where the unavoidable phonon related loss channels can compete with cavity losses, studies of the phonon-influence on these systems has become a major focus of topical research. It has been shown that the QD acoustic phonon coupling is responsible for an unexpectedly strong QD-cavity coupling for cavities that are detuned from the QD resonance [6, 7], which manifests itself in a spectral broadening of the Mollow sidebands through off-resonant cavity emission [8, 9]. Further, it was demonstrated that phonons strongly influence the photon statistics [10–12] and lead to an enhanced coherent scattering as well as to an off-resonant sideband narrowing [8, 13]. Recently, we have performed a numerically complete path-integral analysis dealing with the limiting case of negligible cavity losses and demonstrated that in this case, due to the phonon coupling, an increase of the light-matter coupling can counter-intuitively reduce the visibility of Jaynes-Cummings revivals and lead to a broadening and lowering of spectral sidebands [12].

In this Letter, we demonstrate that the competition of the phonon-induced decoherence with cavity losses brings in qualitatively new aspects to the system dynamics compared to the case when one of the two mechanisms is absent. In particular, the interplay between phonon-induced pure dephasing and phonon-induced renormalizations of the light-matter coupling with cavity and radiative losses strongly and non-trivially affects the transition from the weak to the strong coupling regime as well as Mollow-type spectra, which is manifested in characteristic dependencies on temperature and the light-matter coupling strength. Our analysis combines a microscopic calculation of phonon induced pure dephasing

effects with a phenomenological treatment of other loss channels providing an easy link to the standard analysis of the cross-over between the weak and strong coupling regimes which in the literature is usually discussed without accounting for pure dephasing.

In many typical QD-cavity experiments, the mean photon number is below one. Here, we shall concentrate on this case, which implies that we have to account for the dynamics only in the subspace spanned by the three states: $|0\rangle = |G, n = 0\rangle$, $|1\rangle = |X, n = 0\rangle$ and $|2\rangle = |G, n = 1\rangle$, where G denotes the empty dot without an exciton, while X marks the exciton state. The integer label n refers to the number of photons that are excited in the cavity mode. Other dot states are not considered as they are assumed to be coupled off-resonantly. Using the Jaynes-Cummings model to describe the coupling between the states $|1\rangle$ and $|2\rangle$, closed equations are obtained for the evolution of the density matrix operator $\hat{\rho}_{\ell j} = |\ell\rangle\langle j|$ and the corresponding expectation values $\rho_{\ell j} = \langle \hat{\rho}_{\ell j} \rangle$. The simplest way to account for cavity losses and the dot-environment coupling by radiative decay is to introduce phenomenological rates into the equations of $\rho_{\ell j}$ following the Lindblad formalism as described in standard text books [14]. The goal of the present paper is to provide a clear analysis of the competition of these decay mechanisms with phonon-induced pure dephasing and to characterize the resulting interplay of all loss channels in a comprehensive way.

For a cavity in resonance with the dot transition, a phenomenological model that accounts for all of the above loss channels can be formulated as follows [26]:

$$\frac{d}{dt} \begin{pmatrix} \rho_{11} \\ \rho_{22} \\ V \end{pmatrix} = \underbrace{\begin{pmatrix} -r & 0 & ig \\ 0 & -\kappa & -ig \\ 2i\tilde{g} & -2i\tilde{g} & -(\kappa + r)/2 - \gamma \end{pmatrix}}_{=:M} \begin{pmatrix} \rho_{11} \\ \rho_{22} \\ V \end{pmatrix}, \quad (1)$$

where $V = \rho_{12} - \rho_{21}$. κ accounts for cavity losses and can be expressed in terms of the quality factor Q and the dot transition frequency ω_0 as $\kappa = \omega_0/Q$. r is the radiative decay rate, while γ stands for the phonon-induced

*alexey.vagov@uni-bayreuth.de

pure dephasing. g denotes the bare QD-cavity coupling strength, which in the loss-free case is related to the Rabi frequency Ω by $\Omega = 2g$. Finally, \tilde{g} represent a renormalized light-matter coupling which models the phonon-induced renormalization of the Rabi frequency known from microscopic treatments [7, 12].

The pure dephasing rate γ is introduced according to the Lindblad formalism [13]. Note, that γ , unlike κ and r , does not enter the equations for ρ_{11} and ρ_{22} as pure dephasing alone cannot change occupations [15–17]. The Lindblad formalism, however, does not account for frequency renormalizations. As a phenomenological way to describe these renormalizations, we have introduced \tilde{g} in our model [27].

An overview of the behavior of this dissipative system is most easily obtained by looking at the eigenvalues of the matrix M in Eq. (1). While analytic expressions for these eigenvalues are available, in the general case, when all rates in Eq. (1) are non-zero, they are quite lengthy and not instructive. This is different in two limiting cases. First, when pure dephasing is negligible, i.e., in the limit $\gamma = 0$ and $\tilde{g} = g$, we recover the well known result [18, 19]:

$$\lambda_0 = -\frac{\kappa + r}{2}, \quad \lambda_{\pm} = \lambda_0 \pm \frac{1}{2}\sqrt{(\kappa - r)^2 - 16g^2}. \quad (2)$$

The λ_0 eigenmode decays with the average rate of cavity losses and radiative decay and never shows oscillations. The λ_{\pm} modes become complex for $4g > |\kappa - r|$, i.e., for large enough g , these modes oscillate and exhibit the same g -independent damping as the λ_0 mode. Thus, the λ_{\pm} modes correspond to the side-peaks in Mollow-type spectra, while λ_0 contributes to the unshifted central peak. Eq. (2) predicts that the bifurcation point that separates the weak from the strong coupling regime can even for finite κ be shifted to arbitrarily small values of g when κ and r are similar. However, in typical QD-cavity systems, κ dominates by far.

The second simple limiting case is obtained by setting $\kappa = r = 0$ and keeping γ finite. This situation is usually not discussed, as typically κ cannot be neglected and phonon-induced pure dephasing is regarded to be marginal, especially at low temperatures. Nevertheless, for later comparisons, it is instructive to shortly look at this case, where the eigenvalues are given by

$$\lambda_0 = 0, \quad \lambda_{\pm} = -\frac{\gamma}{2} \pm \frac{1}{2}\sqrt{\gamma^2 - 16g\tilde{g}}, \quad (3)$$

revealing that pure dephasing alone does not damp the λ_0 mode but only the λ_{\pm} modes. For any finite and constant γ , we obtain a well defined bifurcation point at $16g\tilde{g} = \gamma^2$ and for larger $g\tilde{g}$, the damping of the oscillating modes becomes independent of the light-matter coupling and is given by $\gamma/2$.

Interestingly, when κ , r and γ are all non-zero, the situation changes qualitatively compared with the limiting cases of Eqs. (2) and (3), even when we neglect the frequency renormalization and put $\tilde{g} = g$. The green thin

lines in Fig. 1(a) display the eigenvalues of M calculated for $\kappa = 0.1 \text{ ps}^{-1}$, $r = 0.001 \text{ ps}^{-1}$, and $\gamma = 0.01 \text{ ps}^{-1}$ as functions of $g = \tilde{g}$. In contrast to Eqs. (2) and (3), the real parts that correspond to the damping of the modes show a noticeable dependence on g in the strong coupling regime, even though all rates are taken independent on g . In particular, $\text{Re}[\lambda_{\pm}]$ decreases with rising g for g above the bifurcation point. The competition between the different decay channels also strongly affects the position of the bifurcation point. Here, it is essentially only the competition between κ and γ , as r is too small to have a noticeable influence. For the chosen parameters, the bifurcation point is found at $g_b \simeq 0.017 \text{ ps}^{-1}$, which should be compared with the bifurcation point defined by Eq. (2) that is given by $\bar{g}_b = |\kappa - r|/4 \simeq 0.025 \text{ ps}^{-1}$, i.e., adding a constant pure dephasing rate to the cavity loss shifts the bifurcation point to lower values, similar to the effect of a finite value of r in Eq. (2).

So far, our analysis assumed rates that are independent of g . From a microscopic point of view, these assumptions need to be revisited. First of all, pure dephasing is a non-Markovian effect, as can be seen from the fact that the phonon-induced polarization decay after a short pulse excitation is only partial and non-exponential [17]. In this Letter, however, we study the case of a cavity with at most a single photon, which is formally equivalent to a two-level QD without cavity, subject to laser driving with a constant amplitude. Here, the non-Markovian nature of the coupling manifests itself in non-vanishing off-diagonal elements of ρ at long times [20]. However, for resonant driving, the non-vanishing part of ρ_{12} equals $\text{Re}[\rho_{12}]$, which in this case is dynamically decoupled from the three dynamical variables ρ_{11} , ρ_{22} and V appearing in Eq. (1). The phonon-induced pure dephasing has recently been studied for QD-cavity systems [12] within a numerically complete path integral approach [21] in the limit of vanishing cavity and radiative losses. Considering a situation with at most one photon, the dynamics is restricted to a two-level system and it turns out that for a cavity in resonance with the dot transition, the path integral results for the three dynamical variables ρ_{11} , ρ_{22} and V agree perfectly with those obtained from Eqs. (1), provided γ and \tilde{g} are suitably chosen.

In order to extract γ and \tilde{g} from our path integral calculations, we consider the solution for a system initially prepared in the state $|2\rangle$, where the exciton occupation resulting from the simulation can be perfectly described by the formula $\rho_X = \rho_{11} = \frac{1}{2}[1 - e^{-\Gamma t} \cos(\omega t)]$. The fitting parameters Γ and ω depend on g , the temperature T , and the dot parameters that enter the carrier-phonon coupling. Further, it was found from the path integral analysis, that for $\kappa = r = 0$, the system exhibits oscillations for all g . This finding of oscillatory solutions in the microscopic theory for arbitrary small g implies that the g dependent renormalizations of Γ and ω prevent the system from having a crossover to the weak coupling limit, i.e., unlike the theory with a g independent pure dephasing rate [cf. (3)], there is no bifurcation point in a model

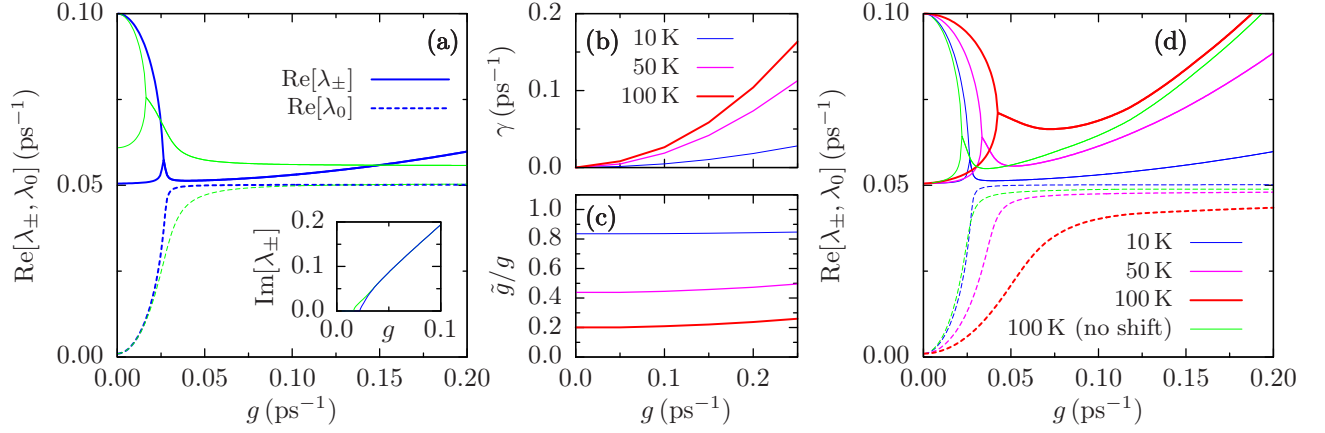


FIG. 1: (Color online) Panel (a): real parts of the eigenvalues of the matrix M in Eq. (1) as a function of the bare light-matter coupling g for $\kappa = 0.1 \text{ ps}^{-1}$ and $r = 0.001 \text{ ps}^{-1}$ assuming a constant pure dephasing rate of $\gamma = 0.01 \text{ ps}^{-1}$ (green thin lines) and using the exact dephasing rate $\gamma(g)$ and accounting for the renormalization $\tilde{g}(g)$ as obtained for a spherical GaAs dot with radius 3 nm at $T = 10 \text{ K}$ (blue thick lines). Inset: corresponding imaginary parts of λ_{\pm} ($\text{Im}[\lambda_0] = 0$, $\text{Im}[\lambda_-] = -\text{Im}[\lambda_+]$). Panels (b) and (c): pure dephasing rate $\gamma(g)$ and renormalization of the light-matter coupling $\tilde{g}(g)/g$ as obtained from exact path integral calculations at three temperatures. Panel (d): real parts of the eigenvalues of the matrix M in Eq. (1) at $T = 10, 50$ and 100 K calculated using the exact damping rate $\gamma(g)$ as well as accounting for the the renormalization $\tilde{g}(g)$ for $\kappa = 0.1 \text{ ps}^{-1}$ and $r = 0.001 \text{ ps}^{-1}$. The green thin line gives results as obtained for $T = 100 \text{ K}$ accounting for $\gamma(g)$ but assuming $\tilde{g} = g$.

where phonon-induced pure dephasing is the only loss channel. From Eq. (3) we learn that for $\kappa = r = 0$, the rate equation Eq. (1) yields the same damped oscillation as the microscopic theory, provided we identify $\gamma = 2\Gamma(g)$ and replace in Eq. (1) the bare light-matter coupling g by $\tilde{g} = [\Gamma^2(g) + \omega^2(g)]/(4g)$.

As the light-matter coupling also enters the radiative recombination rate, r should exhibit a corresponding g dependence, that we will, however, neglect due to the overall smallness of r . Cavity losses on the other hand are mainly properties of the cavity and hence, no significant influence of g is expected. Therefore, we shall in the following use the model in Eq. (1) with $\gamma(g)$ and $\tilde{g}(g)$ determined by our microscopic path-integral approach and keep $\kappa = 0.1 \text{ ps}^{-1}$ and $r = 0.001 \text{ ps}^{-1}$ fixed.

$\gamma(g)$ and $\tilde{g}(g)$ are plotted in Figs. 1(b,c) for a spherical GaAs QD with radius 3 nm and for three temperatures [28]. Most important for our present discussion is that $\gamma(g)$ approaches zero for $g \rightarrow 0$ and rises with rising T , while $\tilde{g}(g)$ exhibits pronounced and strongly T -dependent renormalizations. Accounting for these renormalizations in Eq. (1) has significant consequences on the g dependence of the eigenvalues $\lambda_{\pm,0}$, as demonstrated by the blue thick lines in Fig. 1(a) calculated for $T = 10 \text{ K}$. Most striking is that the bifurcation point is now slightly above the value expected from Eq. (2) (i.e. vanishing phonon influence) and not below as it is expected for a constant γ (cf. the green thin lines). The same trend is seen when looking at the thick lines in Fig. 1(d) that display the eigenvalues $\lambda_{\pm,0}$ for different temperatures accounting for the g dependencies of γ and \tilde{g} . Obviously, the bifurcation point shifts to higher g values with rising temperatures. It is interesting to note, that when only the g dependence of γ is taken into account, the opposite

trend is found [cf. the thin lines in Fig. 1(d)]. The latter result is due to the fact that with rising T , the phonon-induced damping γ increases [cf. Fig. 1(b)] and becomes comparable to κ , resulting in a partial compensation as discussed before for a constant γ in Fig. 1(a) and similar to the competition between κ and r in Eq. (2). However, this partial compensation arising from the competition between κ and $\gamma(g)$ is overcompensated by the renormalization of g , the stronger, the higher the temperature is, and this overcompensation leads to a shift of the bifurcation point towards larger light-matter couplings.

Another striking feature of the full theory with all g -dependent phonon-induced renormalizations is that above the bifurcation point, we now find that the damping of the oscillatory modes λ_{\pm} increases with rising g , which is opposite to the trend seen in calculations with a g -independent γ [green thin lines in Fig. 1(a)]. The g range displayed in Figs. 1(a,d) represents roughly the range of values for g that has been realized in typical state-of-the-art cavities [22, 23]. We note in passing, that when g is further increased, $\text{Re}[\lambda_{\pm}]$ eventually decreases again, mainly due to the non-monotonic g -dependence of γ arising from the resonant nature of the carrier-phonon coupling [12, 24, 25].

Finally, let us turn to the λ_0 mode. Fig. 1(d) clearly shows that the damping of the λ_0 mode increases with rising g , but that it decreases with rising temperature. We stress that this counterintuitive temperature dependence is introduced only by the competition between cavity losses and phonon-induced pure dephasing: cavity losses alone would not lead to a T dependence in our model, as T enters only in the phonon-induced parts. Pure dephasing alone would also not lead to a T dependence, as Eq. (3) predicts no damping of the λ_0 mode at all.

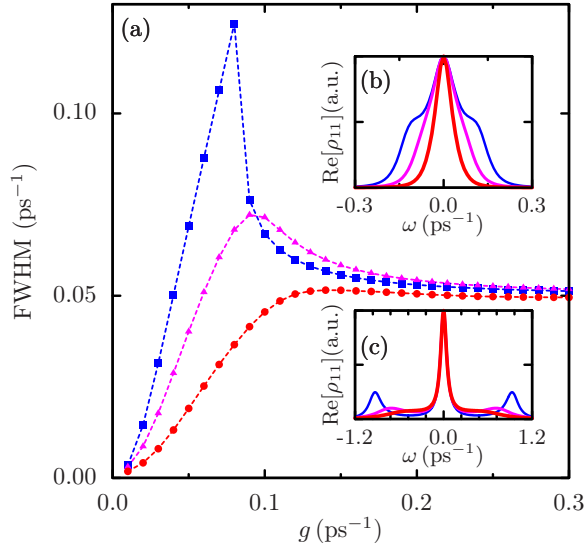


FIG. 2: (Color online) Panel (a): Full width at half maximum (FWHM) of the central peak in the Mollow-type spectra $\text{Re}[\rho_X(\omega)]$ as a function of the light-matter coupling g calculated at $T = 10$ K (blue dashed line with square symbols), $T = 50$ K (purple dashed line with triangles) and $T = 100$ K (red dashed line with circles). Panels (b) and (c): spectra at $T = 10$ (thin blue line), 50 (purple line) and 100 K (thick red line) calculated for (b) $g = 0.075 \text{ ps}^{-1}$ and (c) $g = 0.15 \text{ ps}^{-1}$, respectively. In all panels, $\kappa = 0.1 \text{ ps}^{-1}$ and $r = 0.001 \text{ ps}^{-1}$.

The temperature dependence resulting from the competition between κ and $\gamma(g)$ also affects observable quantities like the Full-Width-at-Half-Maximum (FWHM) of the peak centered at $\omega = 0$ in the spectra $\text{Re}[\rho_X(\omega)]$ that are extracted in Fig. 2(a) as a function of g for different T . It should be noted that also the λ_{\pm} modes contribute to the width of that peak as long as the corresponding frequencies are not well separated from $\omega = 0$

[cf. Figs. 2(b,c)]. For $T = 100$ K, the heights of the side peaks is generally low and thus the FWHM in Fig. 2(a) reflects only the monotonically rising contribution of the λ_0 mode. For lower temperatures, a maximum appears because at low g , the λ_{\pm} contributions strongly enhance the FWHM, while their influence decreases with rising g , when the side peaks move to higher ω and eventually become clearly separated. In the weak coupling limit, the λ_{\pm} contributions are also centered at $\omega = 0$ and their damping typically rises with rising temperature. This trend is, however, overcompensated by the decreasing damping of the λ_0 mode, resulting altogether in a decrease of the FWHM with rising T . Due to the competition between the λ_0 and the λ_{\pm} contributions, the T dependence of the FWHM becomes non-monotonic at intermediate g , while at high g , where the λ_{\pm} modes are not contributing any more, the low g trend, reflecting the dependence of the λ_0 mode, is restored.

In conclusion we have shown that the interplay between cavity losses and the g dependent pure dephasing as well as the phonon-induced renormalization of the bare light-matter coupling strength g strongly affect the transition from the weak to the strong coupling regime, e.g., reflected in T dependent shifts of the bifurcation point. In the weak coupling limit, we predict that the width of the peak at $\omega = 0$ decreases for higher temperatures. Our analysis reveals that the temperature dependence of this line results from the combined action of cavity losses and phonon-induced pure dephasing; both mechanisms alone would lead to a temperature independent width.

We acknowledge fruitful discussions with A. Nazir which helped to more clearly formulate the relation between our phenomenological approach and the microscopic theory. M.D.C. further acknowledges Alexander von Humboldt and BELSPO grants for support.

-
- [1] D. Press, S. Götzinger, S. Reitzenstein, C. Hofmann, A. Löffler, M. Kamp, A. Forchel, and Y. Yamamoto, *Phys. Rev. Lett.* **98**, 117402 (2007).
 - [2] A. Dousse, J. Suffczynski, A. Beveratos, O. Krebs, A. Lemaître, I. Sagnes, J. Bloch, P. Voisin, and P. Senellart, *Nature* **466**, 217 (2010).
 - [3] D. Bouwmeester, A. K. Ekert, and A. Zeilinger, *The Physics of Quantum Information* (Springer, Berlin, 2000).
 - [4] S. Haroche and J. Raimond, *Exploring the quantum* (Oxford University Press, Oxford, 2006), 1st ed.
 - [5] C. Boeckler, S. Reitzenstein, C. Kistner, R. Debusmann, A. Loeffler, T. Kida, S. Hfing, A. Forchel, L. Grenouillet, J. Claudon, et al., *Appl. Phys. Lett.* **92**, 091107 (2008).
 - [6] S. Ates, S. M. Ulrich, A. Ulhaq, S. Reitzenstein, A. Löffler, S. Höfling, A. Forchel, and P. Michler, *Nature Photonics* **3**, 724 (2009).
 - [7] P. Kaer, T. R. Nielsen, P. Lodahl, A. P. Jauho, and J. Mørk, *Phys. Rev. Lett.* **104**, 157401 (2010).
 - [8] S. M. Ulrich, S. Ates, S. Reitzenstein, A. Löffler, A. Forchel, and P. Michler, *Phys. Rev. Lett.* **106**, 247402 (2011).
 - [9] C. Roy and S. Hughes, *Phys. Rev. Lett.* **106**, 247403 (2011).
 - [10] P. Kaer, P. Lodahl, A.-P. Jauho, and J. Mørk, *Phys. Rev. B* **87**, 081308 (2013).
 - [11] Z. Harsij, M. Bagheri Harouni, R. Roknizadeh, and M. H. Naderi, *Phys. Rev. A* **86**, 063803 (2012).
 - [12] M. Glässl, L. Sörgel, A. Vagov, M. D. Croitoru, T. Kuhn, and V. M. Axt, *Phys. Rev. B* **86**, 035319 (2012).
 - [13] D. P. S. McCutcheon and A. Nazir, *Phys. Rev. Lett.* **110**, 217401 (2013).
 - [14] H. P. Breuer and F. Petruccione, *The Theory of Open Quantum Systems* (Oxford University Press, Oxford, 2002), 1st ed.
 - [15] G. D. Mahan, *Many-Particle Physics* (Plenum Press, New York, 1990), 2nd ed.
 - [16] S. Mukamel, *Principles of Nonlinear Optical Spectroscopy*

- (Oxford University Press, New York, Oxford, 1995).
- [17] B. Krummheuer, V. M. Axt, and T. Kuhn, Phys. Rev. B **65**, 195313 (2002).
 - [18] L.C. Andreani, G. Panzarini, and J. M. Gerard, Phys. Rev. B **60**, 13276 (1999).
 - [19] S. Rudin and T. L. Reinecke, Phys. Rev. B **59**, 10227 (1999).
 - [20] M. Glässl, A. Vagov, S. Lüker, D. E. Reiter, M. D. Croitoru, P. Machnikowski, V. M. Axt, and T. Kuhn, Phys. Rev. B **84**, 195311 (2011).
 - [21] A. Vagov, M. D. Croitoru, M. Glässl, V. M. Axt, and T. Kuhn, Phys. Rev. B **83**, 094303 (2011).
 - [22] J. P. Reithmaier, G. Sek, A. Löffler, C. Hofmann, S. Kuhn, S. Reitzenstein, L. V. Keldysh, V. D. Kulakovskii, T. L. Reinecke, and A. Forchel, Nature **432**, 197 (2004).
 - [23] K. Hennessy, A. Badolato, M. Winger, D. Gerace, M. Atatüre, S. Gulde, S. Fält, E. L. Hu, and A. Imamoglu, Nature **445**, 896 (2007).
 - [24] P. Machnikowski and L. Jacak, Phys. Rev. B **69**, 193302 (2004).
 - [25] A. Vagov, M. D. Croitoru, V. M. Axt, T. Kuhn, and F. M. Peeters, Phys. Rev. Lett. **98**, 227403 (2007).
 - [26] The dynamics of the density matrix elements involving the ground state $|0\rangle$ do not couple back to the above variables and thus need not to be considered here.
 - [27] In accordance with the microscopic treatment, the phonon-induced modifications enter only in the equation for the off-diagonal density matrix elements.
 - [28] The carrier-phonon coupling constants are taken from Ref. 17